View metadata, citation and similar papers at core.ac.uk

brought to you by CORE

provided by ROS: The Research Output Service. Heriot-Watt University Edinburgh

ACADEMIC REGISTRY

Research Thesis Submission

Name:	STEPHEN WILLIAM GIERTHY		
School/PGI:	INSTITUTE OF BIOCHEMISTRY, BIOPHYSICS AND BIOENGINEERING (IB3)		
Version: *(i.e. First, Resubmission, Final)*	FINAL	Degree Sought (Award **and** Subject area)	MSC BY RESEARCH

Declaration

In accordance with the appropriate regulations I hereby submit my thesis and I declare that:

1) the thesis embodies the results of my own work and has been composed by myself
2) where appropriate, I have made acknowledgement of the work of others and have made reference to work carried out in collaboration with other persons
3) the thesis is the correct version of the thesis for submission and is the same version as any electronic versions submitted*.
4) my thesis for the award referred to, deposited in the Heriot-Watt University Library, should be made available for loan or photocopying and be available via the Institutional Repository, subject to such conditions as the Librarian may require
5) I understand that as a student of the University I am required to abide by the Regulations of the University and to conform to its discipline.

* *Please note that it is the responsibility of the candidate to ensure that the correct version of the thesis is submitted.*

Signature of Candidate:		Date:	

Submission

Submitted By *(name in capitals):*	STEPHEN WILLIAM GIERTHY
Signature of Individual Submitting:	
Date Submitted:	

For Completion in the Student Service Centre (SSC)

Received in the SSC by *(name in capitals):*			
Method of Submission *(Handed in to SSC; posted through internal/external mail):*			
E-thesis Submitted **(mandatory for final theses)**			
Signature:		Date:	

Functionally Tailored Materials for Medical Devices

Development of a biocompatible shape memory alloy

MSc by Research thesis

Author: Stephen William Gierthy

Project supervisors: Dr. Carmen Torres-Sanchez & Dr. Theodore Lim

Research carried out in Heriot Watt University

TABLE OF CONTENTS

ABSTRACT

Medical devices are constructs created to aid patients who suffer from medical problems, such as health problems regarding arteries in the heart, to patients who have been born with congenital absence, or have become an amputee through disease or trauma. Material selection plays an important role when developing these forms of medical devices, as the materials are required to have the mechanical properties to allow the device to operate with its intended function but also be biocompatible to be used in conjunction with human physiology.

Through a literature review, this thesis explores materials and their associated mechanics currently used in medical devices and details other possible materials which could be used that could significantly improve the ability of the device. The review will give particular scope to intelligent materials which could be incorporated into medical devices which could potentially allow the device to grow.

This thesis will concentrate on alloy configurations to develop an intelligent material called a shape memory alloy. A shape memory alloy is an alloy type which can ‘remember’ and return to original shapes when deformed. Through the use of element composition and development procedures used to create the alloy, the alloy could be manipulated to potentially simulate growth by remembering its original grown form when deformed into a smaller collapsed form.

A biocompatible shape memory alloy, Ti-7.5Nb-4Mo-1Sn, has been shown to have shape memory alloy properties (superelasticity and shape memory effect) at low temperatures, around room temperature (20-25°C) and is deemed a suitable starting alloy to re-create and adapt by changing the elemental composition - in particular the more beta stabilising elements Nb and Mo - and development protocols used which will change the alloys phase transformation temperatures so the alloys could change crystal structure showing shape memory effect at human body temperature (37°C) which would allow it to grow by expanding when used in conjunction with a medical devices.

The results of the thesis show that Nb has the greatest effect on changing the alloys transformation temperatures, with more Nb amounts moving the temperatures into the 30°C range. Mo is shown to make the alloys more superelastic and also move the transformation temperature and the Sn is shown to make the alloy stronger which is required for use in medical devices that are used with human physiology.

1 INTRODUCTION

The following thesis is the summation of the work carried out for an MSc by Research project, which involves the development of an intelligent material aimed to be integrated with medical devices providing them the ability to self-expand.

The main work carried out within the research is from a material science perspective, where shape memory materials and their mechanical properties have been researched to see if it would be possible to have a material which could self-expand, by expanding to larger dimensions from an original smaller dimension. The material would then be incorporated into medical devices (such as stents, replacement bones and prosthetic medical devices) to allow the device to grow in proportion to the natural growth of the user.

This thesis begins with a literature review that explores shape memory materials called shape memory alloys which have been created for use in medical devices. Shape memory alloys are alloys which can be deformed from an original shape and return to its pre-deformed shape through phase transformation stimulated by an energy source. The end aim of this thesis is to use human body temperature (37°C [1]) as the energy source which would affect the phase change properties of the shape memory alloy for the medical devices, allowing it to expand when compressed to a smaller shrunk form and therefore simulate growth by returning to its original full size before deformation.

A shape memory alloy chosen from literature has been shown to have shape memory properties around room temperature (20-25°C [2, 3]) as it exhibits superelasticity and shape memory effect as it is deformed by mechanical testing. The thesis continues by recreating this shape memory alloy alongside variations of the alloy which is done through compositional, creation development through how the elements are fused together and mechanical testing experimentation, to see if it is possible to alter the characteristics of this alloy so it has shape memory properties around human body temperatures.

To conclude, a future work plan is discussed which outlines further development methods to continue the research as well as a possible energy harvesting device which would take the heat from the human body and apply it to the material: where both the alloy and harvest system would work in conjunction to allow the material to expand under controlled circumstances and therefore allow the medical device to expand, simulating growth.

2 LITERATURE REVIEW

The following literature review will focus on titanium based shape memory alloys exploring the effect of the β-stabilising elements in their respective compositions have on the mechanical properties of the alloy. The elements used in the alloys are nickel free and biocompatible with human physiology. Most of the alloys reviewed are suitable for biomedical applications, that is, the alloys are capable of phase changes with shape memory properties (shape memory effect and superelasticity) at low temperatures: room temperature to body temperature (293-310K or 20-37°C, respectively [1, 2]).

β-type shape memory behaviour is due to the reversible martensitic transformation between the β parent phase and the α'' martensitic phase [4]. This β phase is achieved through the addition of β phase stabilising elements, such as nickel (Ni), tantalum (Ta), niobium (Nb), molybdenum (Mo) and tin (Sn). This is due to the desirable properties these types of alloys present, such as high corrosion resistance, strength, durability, ease of workability and biocompatibility [5].

The most well-known titanium based shape memory alloy is nickel-titanium (Ni-Ti). However, nickel may not be suitable for use in biomedical applications as it has been shown to cause hypersensitivity with nickel sensitive patients, as well as reports of *in vivo* human and animal studies which report that nickel is a potential carcinogen [6-8].

Extensive studies have subsequently been conducted into nickel free shape memory alloys which have shape memory and superelastic behaviour at human body temperature in order for them to be utilised in biomedical devices and used in conjunction human physiology.

2.1 Ti-Ta SMAs

Titanium-tantalum (Ti-Ta) shape memory alloys were investigated by [4] which reported shape memory effect in Ti-(30-40)Ta alloys. The study reveals that martensitic transformation start temperature (Ms) is decreased by 30K for every 1at.% addition of Ta in the composition.

Ti-(30-40)Ta ingots were prepared by arc-melting in an argon atmosphere. The ingots were the homogenised at 1273K (~1000°C) for 2 hours before being cut by spark-erosion cutting machinery. The samples were solution-treated at 1173K (~900°C) for 30 minutes before finally quenched into water. Some specimens were further aged at 573K (~300°C).

Shape memory behaviour was determined through tensile testing at various constant stresses during thermal cycling applied in 50MPa increments. Phase formation was determined by X-ray diffraction (XRD) at room temperature.

Solution-treated and water quenched Ti-(30-40)Ta XRD profiles at room temperature identified body-centred cubic β phase structure and disordered orthorhombic α'' phase peaks in the alloys. Ti-(30 and 32)Ta exhibited only α'' phase, Ti-36Ta exhibited β and α'' phase and Ti-40Ta exhibited only β phase. The study suggests that composition has a vital role on

martensitic transformation temperatures, where samples exhibiting α'' phase have Ms above room temperature and those exhibiting β phase have Ms below room temperature.

XRD profiles at room temperature of solution-treated Ti-32Ta alloys before aging showed only α'' phase which the study states is due to Mf temperature being above room temperature. Aged alloys at 573K for 1 hour showed both α'' and β phase, which the study says indicates that aging decreased the transformation temperatures.

From strain-temperature curves obtained from tensile testing at various constant stresses during thermal cycling, shape memory effect was confirmed in all alloys. Specimens elongated due to martensitic transformation during cooling and strain recovered due to reverse transformation during heating. Ti-40Ta at 50MPa was shown to have an Ms temperature of 260K (~-13°C), which explains the single β phase from the XRD profile. For an overall view of the effect Ta has, the study plotted Ms and Af temperatures in terms of temperature against Ta content, where both Ms and Af decreased by approximately 30K every 1at.% addition of Ta.

Shape memory effect was confirmed during thermal cycle testing between 173-513K (~-100-240°C), for Ti-32Ta alloy, which exhibited Ms and Af temperatures of 440K (~166°C) and 485K (~212°C), respectively, during the first cycle; which temperature decreased gradually as the number of cycles increased. Increasing the cycling temperatures from 173-573K for the same alloy, Ms temperature was again 440K after the first cycle, but reduced significantly to 380K (~106°C) after the fifth cycle. A sample was aged after the first cycle at 573K for 1 hour and during the second cycle, the alloy had an Ms of 380K, which the study suggests is the alloy undergoing phase decomposition.

The study compared thermal stability of the Ti-Ta alloys in comparison to Ti-Nb alloys. The study chose Ti-22Nb from previous reports in which the alloy was expected to have an Ms temperature above 373K (~100°C). From strain-temperature curves of the Ti-22Nb alloy, shape memory effect was confirmed after the first thermal cycle (cycles between 173-513K under constant stress of 50MPa) with Ms temperature of 420K (~146°C) and Af temperature of 470K (~197°C), which is close to the transformation temperatures of Ti-32Ta described above. However, unlike Ti-32Ta, after the second cycle, Ti-22Nb did not reveal shape memory effect, which the study implies the alloy would be unstable with thermal cycling. Increasing the thermal cycle range to 173-573K "completely supressed the shape memory effect" of the alloy during the first cycle.

The study refers to Ta as a "weak β-stabilizer" when compared to other stabilising elements such as niobium (Nb) and molybdenum (Mo). However, Ta was shown to be far superior for high temperature shape memory alloy applications than Nb and possibly not suitable for the lower temperatures required for biomedical applications. The study notes the effect aging has on the alloys transformation temperatures.

2.2 Ti-Nb SMAs

Titanium-niobium (Ti-Nb) shape memory alloys were explored by [9] which aimed to develop a nickel free shape memory alloy suitable for biomedical applications by experimenting with Ti-(20-29)at.%Nb alloys. It is confirmed that at room temperature, shape memory effect was noted in a Ti-(22-25)at.%Nb alloy and superelastic behaviour was noted in a Ti-(25.5-27)at.%Nb alloy.

Experiments with the Ti-Nb alloys were conducted using tensile tests carried out at a strain rate of $1.67x10^{-4}s^{-1}$ at varying temperatures, as well as thermal cycling tests at constant stresses.

Ti-(20-29)at.%Nb alloys were prepared by argon arc-melting. The ingots were heat-treated between 573K-1273K (~300-1000°C) for 60 seconds to 1 hour, respectively. The treated ingots were quenched into water and test samples were cut into 20mm lengths by an electro-discharge machine, with any surface damage removed by mechanical polishing. XRD testing was conducted to determine phase at room temperature with CuKα radiation.

The tensile stress-strain curves results at room temperature for the Ti-(20-28)at.%Nb alloy solution-treated at 1173K (~900°C) for 30 minutes, reported that Ti-20at.%Nb exhibited the largest elongation of 40%. This was shown to decrease with increasing Nb content. Ti-28at%Nb exhibited yielding and Ti-26at%Nb exhibited double yielding. The study suggests that the increased yield stress as the Nb amount is reduced, with lack of superelastic behaviour, was due to the "increase of stress for the reorientation of martensite variants", meaning the stress for inducing martensite is higher in the Ti-(28-29)at%Nb alloys than the slip deformation due to dislocations.

After unloaded from a strain of ~2.5%, Ti-(22-29)at.%Nb alloys were heated to ~500K (~227°C). Ti-(22-25)at.%Nb confirmed shape memory effect and Ti-(25.5-27)at.%Nb confirmed superelastic properties, with Ti-26at%Nb showing the largest strain recovered superelastically. Ti-(28-29)at.%Nb did not exhibit any shape memory effect or superelastic behaviour.

Thermal cycling test results for the solution-treated Ti-26at.%Nb alloy were conducted at temperatures between 173-423K (~-100-150°C) under constant stresses. The study noted the transformation temperatures (martensitic transformations (Ms/ Mf) and reverse transformations (As/ Af) from the graphs and plotted the Ms temperatures for solution treated Ti-(25-28)at.%Nb alloys against Nb content. Temperature showing the minimum critical stress was taken to be the Ms temperature and the study reports Ms temperature having a linear decrease with increasing Nb content of roughly 43K per 1at.% addition of Nb.

XRD profiles of Ti-(20,24,and 28)at.%Nb alloys noted peaks of single phase of disordered BCC (β) in Ti-28at%Nb at room temperature, indicating that Ms temperature is lower than room temperature. Orthorhombic martensite (α'') and β peaks were noted from Ti-24at% alloy and purely α'' peaks were observed in Ti-20at%Nb, indicating that the Mf temperature is higher than room temperature.

From stress-strain curves at varying temperatures, 77-353K (~-176-80°C), for the solution treated Ti-26at.%Nb alloy, shape memory effect was observed in the alloys when deformed between 77-273K, with fully recovered residual strain after unloading by heating the alloys to about 500K. Superelastic behaviour was noted at 293K and 313K (~20°C and 40°C) with largest superelastic strain at 293K.

The study has shown that solution-treated Ti-(25-26)at.%Nb alloys are capable of superelastic behaviour and transformation temperatures at temperatures close to human body temperature. Ti-26a.t%Nb alloys have shape memory behaviour at low temperatures close to 0°C, overall suggesting that the Nb content has a critical effect on the Ms temperature of Ti-Nb alloys.

2.3 Ti-Nb-Sn SMAs

Titanium-niobium-tin (TiNbSn) shape memory alloy were investigated by [5] to determine the superelasticity of the alloys for biomedical applications by experimenting with Ti-16at.%Nb-4.8at.%Sn alloys. The study found that Ti-16Nb-4.8Sn has a reverse martensitic transformation finish temperature (Af) at 266K (~-7°C) and exhibits superelasticity, with an elastic recovery stain of 3.2% at around human body temperature, 310K (~37°C).

Ti-16at.%Nb-(4, 4.7, and 4.9)at.%Sn alloys were argon arc- melted. The ingots were homogenised at 1423K (~1150°C) for 24 hours. Samples were cold rolled and cut by an electro-discharge machine to dimensions of 50x10x1mm for Young's Modulus testing and dimensions of 20x 3x0.2mm for tensile testing. Samples were encapsulated in a vacuum sealed quartz tube and solution treated at 923K (~650°C) for 30 minutes, before quenched into ice water. Some samples were then aged at 333-423K (~60-150°C) for varying times.

The study refers to similarities between itself and a Ti-Ni alloy previously experimented with (Miyazaki *et al [10]*) which states that the transformation temperature decreases rapidly with increasing Ni content. Large superelastic strain recovery with almost no residual strain was found in the Ti-Ni alloy at temperatures around 25-50K higher than the reverse martensitic finish temperature (Af), whereas this study observed large recoverable strain at temperatures 40-50K higher than Af.

The results of the tensile stress-strain curves of the quenched Ti-16Nb-4.8Sn alloy at varying temperatures, 253-373K (~-20-100°C), where specimens were loaded/ unloaded with increasing maximum applied strain of 2-5%, noted that TiNbSn alloys were been found to "undergo thermoplastic martensitic transformation". That is, the elastic results from 253-333K are due to stress inducing martensitic transformation with the total strain recovery due to reverse martensitic transformation (superelasticity). At 310K (~37°C, human body temperature) almost complete recovery is observed at an applied strain of 3% in these alloys.

Titanium-niobium-tin, powders were experimented by [11] to investigate the phase transformation during milling for varying times using a high energy ball milling machine for an alloy composition of Ti-35Nb-2.5Sn. Nb was selected as the β-stabilising element and Sn

as a reducer of the elastic modulus (reduces Young's Modulus and increases tensile strength). The powders were mixed for 24 hours in a mixing machine and then ball milled for 1-12 hours in the high energy ball milling machine. Particle sizes and phases of powders were analysed using XRD, scanning electron microscope (SEM) and particle size distribution (PSD). Titanium was found to be fully transformed from α phase to β phase after 12 hours of milling.

Ti, Nb and Sn powders were mixed for 24 hours using a low speed mixing machine. The powders were then placed into a stainless steel vial with stainless steel balls (with ratio 4:1). The vial was sealed in a box in an argon atmosphere. The milling was conducted at room temperature for the different milling times. Samples of the powders were sent for XRD and the particle size changes were analysed by SEM at 15-25kV. Samples were thermally analysed with differential thermal analysis (DTA) using a flow of argon gas.

XRD profiles were taken to explore the phase changes during milling at different times for the Ti-35Nb-2.5Sn as-mixed powder composition. The XRD pattern identifies only a mixture of α phase Ti, Nb and Sn, which was assumed, as no actual mechanical processing had taken place. After milling for 1 hour, the same α peaks were noted but were found to have decreased intensity of α Ti. After 12 hours milling time, α Ti had disappeared as well as the Sn peaks. After 12 hours, all peaks had turned to β Ti, forming a solid solution with Nb, indicating α Ti/ Nb with identical lattice and atom dimensions. The average particle size of the Ti-35Nb-2.5Sn showed a reduction with milling time, from 46nm-7nm after 12 hours.

SEM micrographs indicated that the particle size decreased with increasing milling time, gradually reducing from 15μm to 7μm after 12 hours. The backscattered SEM micrographs of the as-mixed powders reported Sn particles surrounded by Ti and Nb particles, which Sn particles reduced after 1 hour of milling. After 4 hours, Sn particles completely disappeared which the study indicates that a solid solution of Ti and Nb was formed; all of which is in agreement to the XRD results. Finally the SEM micrographs indicated that the homogeneity of the powders increased as the particles decreased in size due to the increasing milling time.

PSD analysis was used to analyse the particle size of the as-mixed and milled powders during different milling times. The average particle sizes of the elements were reduced from 86-9nm from as-mixed to 12 hour milled samples, which is in agreement with XRD powder size results. The study suggested that the difference in size compared to the SEM results were due to different equipment and measuring sensitivities.

The study confirmed that milling powders can aid in changing phase of the alloys prior to fusing together, where, the milling time has the largest effect on promoting phase change.

2.4 Ti-Mo-Sn SMAs

Titanium-molybdenum-tin (Ti-Mo-Sn) alloys were explored by [12] to be a substitute for titanium-nickel (Ti-Ni) alloys for biomedical applications, giving particular scope to heat treatment effect on shape memory and superelastic behaviour of the alloys. The study finds that shape memory effect is enhanced by aging a Ti-5mol%Mo-4mol%Sn alloy at 873K (~600°C) for 3-7 minutes. The study also finds that superelasticity is improved by aging a Ti-

5mol%Mo-5mol%Sn alloy at 873K (~600°C) for 3-5 minutes, which alloy also exhibits a recovery strain of 3.5% at room temperature when aged at 873K (~600°C) for 5 minutes due to improvement of superelasticity from an increment in the recovery strain with reverse transformation of stress induced martensite.

The study explains that previous experiments with TiMoSn alloys, the Sn content reduces the martensitic transformation temperature as the Sn content is increased [13]. For this particular study, the superelasticity is more applicable than shape memory effect, which happens at body temperature in a Ti-5Mo-XSn where X is greater than 4mol%Sn. Convenient bending tests were conducted at room temperature to determine shape memory properties and tensile testing under a strain rate of $4.16x10^{-4}s^{-1}$ at room temperature were conducted to determine superelasticity.

Ti-5mol%Mo-(4-5)mol%Sn ingots were argon arc-melted. They were homogenised at 1373K (~1100°C) for 24 hours and cold rolled into 0.4mm thickness before being solution-treated at 1273K (~1000°C) for 30 minutes, followed by quenching into ice water. Some alloys were then aged at 873K for varying times which the study reports were determined by preliminary experiments.

Figure 2.1 below shows the Ti-5Mo-4Sn solution-treated and solution-treated then aged alloys results from the convenient bending tests, with the solution-treated then aged alloys demonstrating shape memory effect after heating.

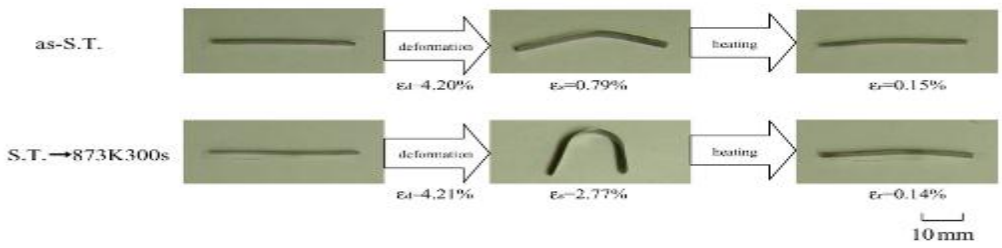

Figure 2.1 - Ti-5Mo-4Sn convenient bending results [12]

The study reports that the recovery ratio with shape memory effect (Rsme) and recovery ratio with spring back after bending deformation (the superelastic property of the alloy (Rsb)) can be defined by the following equations:

$$Rsme = \frac{\varepsilon s - \varepsilon r}{\varepsilon d} x100(\%)$$

$$Rsb = \frac{\varepsilon d - \varepsilon s}{\varepsilon d} x100(\%)$$

Where:

- εs is the surface strain after bending deformation.
- εr is the residual surface strain after heating.
- εd is the applied surface strain with bending deformation.

The increasing aging time of the Ti-5Mo-4Sn alloys causes Rsb to decreases and Rsme to increases, which promotes shape memory effect. Ti-5Mo-5Sn demonstrates more superelasticity due to the increasing Rsb.

Investigating the superelasticity further, from loading/ unloading cyclic tests, superelasticity properties are more promentant in the Ti-5Mo-5Sn alloy solution-treated then aged at 873K for 5 minutes which shows a maximum strain of 3.5% in comparison to 3% the solution-treated alone; when under an applied strain of 5%.

The study refers to the reverse transformation of stress induced martensite as ε_{SIMT} and total recovery strain with superelasticity as ε_{SE}. The solution-treated alloy shows an increase in ε_{SIMT} until 4% applied strain followed by a decrease, whereas the aged alloy ε_{SIMT} increases with increasing applied strain up to 5%. ε_{SE} in the aged alloy is affected by the increase of ε_{SIMT}: superelasticity in the aged Ti-5Mo-5Sn alloy is affected by the recovery strain associated with the reverse transformation of stress induced martensite.

The stress-strain curves obtained at various temperatures for the solution-treated and aged Ti-5Mo-5Sn alloys. Although superelasticity is noted at all test temperatures, it is more recognisable in the aged alloys, with near perfect superelasticity at 223K (-50°C). The study suggests that superelasticity appears most significantly at temperatures 10-20K higher than Af, so for biomedical applications, Af temperature should be increased.

2.5 Ti-Nb-Mo-Sn SMAs

Titanium-niobium-molybdenum-tin shape memory alloys were studied by [14] which aimed to explore the shape memory and superelastic behaviour of a Ti-based shape memory alloy with composition Ti-7.5Nb-4Mo-1Sn which the study reports was determined theoretically. Results showed that the martensitic transformation temperature of the alloy is near 261K (~-12°C) but through tensile and thermal cycling testing, also showed that the alloy exhibits stable shape memory properties and superelasticity at room temperature.

Ti-7.5Nb-4Mo-1Sn alloys were arc-melted in an argon atmosphere, cut by electro-discharge machinery into 1x2x8mm samples and solution-treated at 1273K (1000°C) for 30 minutes followed by quenching into ice water. XRD was conducted on the samples at room temperature and phase transformation was determined by DSC.

From stress-strain results of the alloy at room temperature, the alloys exhibited a two-stage yielding (at 460MPa and 640MPa) behaviour which the study implies shows the alloy has shape memory effect or superelasticity at room temperature.

The study reports that from the XRD profiles of the samples, before and after they were deformed, α-phase cannot be observed before deformation, with only β-phase present, which insinuates that the Ms of the alloy is below room temperature. With a deformation of 22%, α'' appear, implying that deformation is inducing martensitic transformation of β->α'', which results in the double yielding.

DSC results reported an endothermic peak at 273K (~0°C) on heating, representing α''->β and an exothermic peak at 261K on cooling, representing β->α'', stating the martensitic transformation temperature about 261K below room temperature.

The study states shape memory behaviour of the alloy can be define as:

- ε_P, permanently remained strain after unloading.
- ε_E, strain recovered elastically upon unloading.
- ε_{Tr}, recovered strain due to reverse transformation as well as superelastically recovered strain and strain recovered by heating.
- ε_{Tot}, total recovered strain ($\varepsilon_{Tr} + \varepsilon_E$).
- σ_{SIM}, Martensitic transformation stress.

This is shown graphically in Figure 2.2 below.

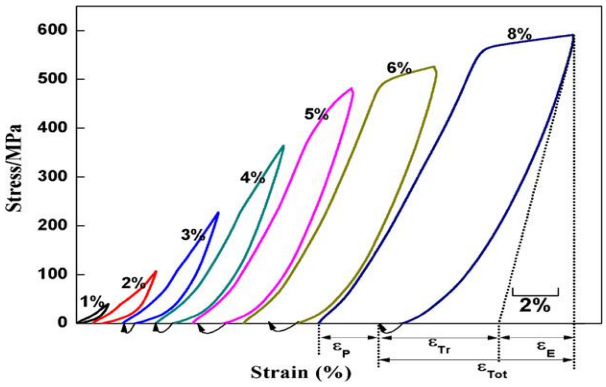

Figure 2.2 - Ti-7.5Nb-4Mo-1Sn tensile results [14]

Near complete superelastic recovery is observable in the first four curves, where after the fifth curve, recovery is achieved through heating above Af temperature. ε_P increases with increasing applied strain from 6%.

The superelasticity stability of the alloys at room temperature was tested through loading/ unloading cyclic tensile test results up to 5% strain. Plastic strain and therefore incomplete superelasticity is observed in the first four cycles with almost complete superelasticity observed with narrow stress hysteresis in the fifth and further cycles. Stress for inducing martensitic transformation causing the yield stress decreases as the cyclic numbers increase, which implies the alloy exhibits stable superelasticity at room temperature.

This alloy was chosen to investigate further as each element has been shown through the studies to have an important effect on the superelasticity and shape memory effect of the alloy. As the alloy has also shown to have transformation temperatures at room temperature, through experimenting with the composition and development through how the alloys are fused, this thesis will aim to change the transformation temperature of the alloy to bring them closer to human body temperature for medical device use.

3 DEVELOPMENT OF BIOCOMPATIBLE SHAPE MEMORY ALLOY

The following section describes the methodology and development stages in replicating the Ti-7.5Nb-4Mo-1Sn (at.%) (TNMS) biocompatible SMA using similar techniques as described in the literature review. This will be the template used to create an alloy with shape memory properties and transformation temperatures at human body temperature.

3.1 Powder homogenisation methodology

APPENDIX A describes how the Ti-7.5Nb-4Mo-1Sn composition was created. The composition powders were mechanically alloyed using a Fritsch Planetary Mono Mill Pulverissette 6 ball miller. Ball milling was used to homogenise the metal powders, as this mechanical alloying process has been known to improve mechanical properties of the alloys [11, 15].

The ball millers' manual [16], suggested the following milling parameters:

- Longer milling time and higher speed (RPM) would result in finer powder particles.
- Initialising the reverse option would promote better alloying; ensuring the powder elements meshed together.
- Powders should be milled in an argon rich atmosphere to prevent oxides.
- Ball to powder weight should be of a ratio of 10:1.

For the composition of weight 3.8414g, 10 balls were used. The balls were placed into the grinding bowl and composition powder emptied on top. A gassing lid was fitted onto the top of the bowl, using rubber seals to keep the gas during milling. The bowl was placed into a clamping rig system and installed into the miller. Argon gas was pumped into the grinding bowl and air was purged from the bowl to ensure that the powders were milled in an inert atmosphere. The miller was set to a 12 hour milling time, with 200RPM speed: these milling parameters came from [17], which ball mill similar TiNbSn metal powders.

Figure 3.1 below shows the setup stages and final homogenised powders from ball milling.

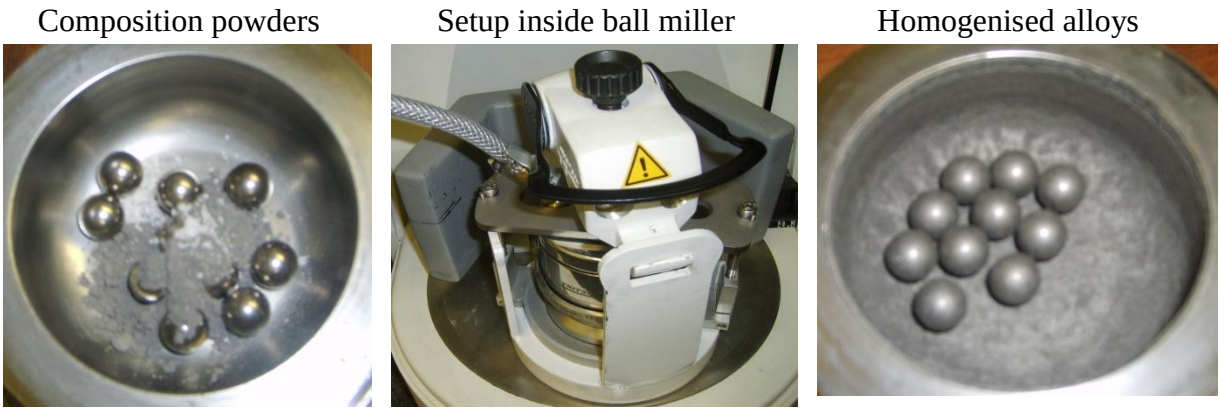

Figure 3.1 - Powders before, during and after milling

3.2 Pressing methodology

Before melting the alloys, the homogenised powders were first pressed into cylindrical ingot shapes. A Denison press was used to press the powders. A pressure of 250MPa (~19kN), taken from [17], was used to press the powders.

The mould, shown in Figure 3.2 below, made from stainless steel, created cylindrical ingots of approximately 1cm diameter and 5mm height. The mould had a circular base with protruding top, in which an outer sleeve could be housed around to keep an inner sleeve from moving during pressing. The inner sleeve had a central hole through it into which the powder was poured. A central pillar would slot through the inner sleeve and press the power inside.

Figure 3.2 - Pressing mould

Powders were pressed before fusion to ingot form so they could be mechanically tested with regards to the dimensions of the ingot. The moulds used for this experiment only produced cylindrical ingots, which could only be compression tested; but in order to observe the full mechanical properties, the alloys would require to be tested by tensile and destructive forces.

Figure 3.3 - Universal mould, compression (left), tensile (middle), destructive (right)

below shows a rough proposed design of a universal mould, which would be capable of producing the ingots for testing and be made from hardened steel, with the pillar holes inside honed to help with pressing. The new moulds would operate similarly as the current mould does, except they would create three different shapes.

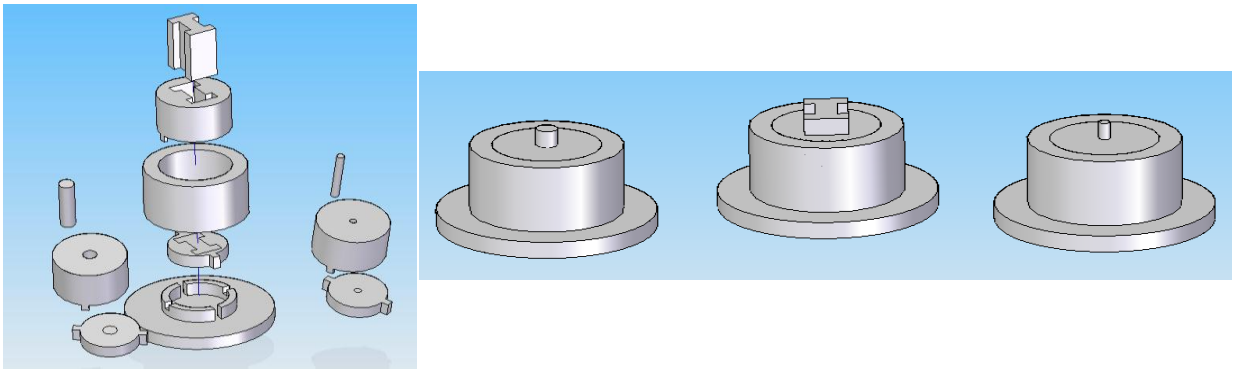

Figure 3.3 - Universal mould, compression (left), tensile (middle), destructive (right)

3.3 Fusion process: sintering

A Lenton sintering furnace was used to sinter the powders in an argon atmosphere. Ingots were placed on a ceramic boat and inserted into the centre of the furnace. A metal O-ring and gas inlet tube were attached and gas inlet tube pumped argon into the furnace at roughly 5PSI. A gas extraction tube removed the argon from the furnace, passing through copper tubes to cool the gas on its way out.

The ingots had their temperature ramped up from roughly room temperature to a specific temperature over a set period of time, which they will dwell at for another period time. Gradually, they are left to cool. The sintering temperatures and times were taken from [17], where the alloys would be ramped up to 1000°C (to allow for phase transition) at a rate of 5°C per minute and then dwelled at 1000°C for 180 minutes, before being cooled down to room temperature at 35°C per minute.

3.4 Fusion process: arc-melting

An Edmund Buhler MAM1 arc-melter was used to arc-melt the powders in an argon atmosphere. All arc-melted samples were melted by a chemistry PhD student, Ruth Downie, where the following was the methodology employed.

- Alloys were loaded into the arc-melter chamber along with a lump of zirconium (Zr);
    - The Zr acts as a ‘getter’ and when melted, removes any remaining oxygen.
- Oxygen was removed from the chamber and then filled with argon: repeated 3 times;
- The chamber was then evacuated and filled with argon until the pressure was just less than atmospheric pressure;
- Water was introduced to flow through the system in order to keep the copper base plate and tungsten electrode cool;
- The arc-melter was set to ‘3’ which was first used to melt the Zr lump and the discharge from the electrode melted the alloys;
- The melter was left for 5 minutes to allow the system to cool down and air was re-admitted to the system as the alloys were removed;
- The alloys were flipped over and the whole process was repeated, to ensure full melt;
- For the second melt, the arc-melter was set to ‘6’ and samples were melted again.

3.5 Mechanical test methodology

Both sintered and arc-melted alloys had their mechanical properties examined by compression mechanical testing which was carried out on an Instron testing machines.

The Instron 3367 was used to vary the loads (1-8% compressive strains) acting upon the alloys at various temperatures: room temperature 20-25°C, less than 14°C, human body temperature 37°C and greater than 50°C.

Stress-strain graphs were produced from each test and maximum achieved stresses (strength of the alloy) and residual strains (elasticity) were calculated from the graphs. Alloys were placed upon the plates of the testing machine and the top plate was lowered till just touching the alloy and machine variables reset to zero at this point. A heating element wrapped in an insulating cloth was wound around these plates and would allow the alloy to be tested at various temperatures.

An Instron 5567 was used to apply an incremental load of 500N from 500-2.5kN at a constant temperature. The reverse was carried out by applying a constant load and varying the temperatures in 5°C increments to show the transformation temperature characteristics.

Different compositions of the original Ti-7.5Nb-4Mo-1Sn (TNMS) alloy were developed for testing. The alloy compositions were chosen as 50% less and 50% greater than the original amount so the results could show what effects each element was having on the entire composition, where compositions are listed in Table 1 below.

Table 1 - Compositions

Changing element	Composition (at.%)	Denoted as
	Ti-7.5Nb-4Mo-1Sn	TNMS
Nb	Ti-5Nb-4Mo-1Sn	5Nb
Nb	Ti-10Nb-4Mo-1Sn	10Nb
Mo	Ti-7.5Nb-2Mo-1Sn	2Mo
Mo	Ti-7.5Nb-6Mo-1Sn	6Mo
Sn	Ti-7.5Nb-4Mo-0.5Sn	0.5Sn
Sn	Ti-7.5Nb-4Mo-2Sn	2Sn

4 RESULTS

The following are the mechanical results of the different fusion and compositions of alloys. Results are from varying compressive strain at constant temperatures, increasing loads at constant temperature and constant loading at varying temperatures. Maximum stress is calculated by the compression force from the Instron machine acting over the area of the alloys and residual strain is calculated by extension caused by the compression of the alloy from the alloys original height.

4.1 Compressive strain at room temperature results

Ti-7.5Nb-4Mo-1Sn will be referred to as TNMS.

Table 2 - TNMS sintered and arc-melted dimensions

Alloy name	Composition (at.%)	Height (mm)	Diameter (mm)
TNMS Sint.	Ti-7.5Nb-4Mo-1Sn	5.54	8.71
TNMS Arc	Ti-7.5Nb-4Mo-1Sn	5.18	9.83

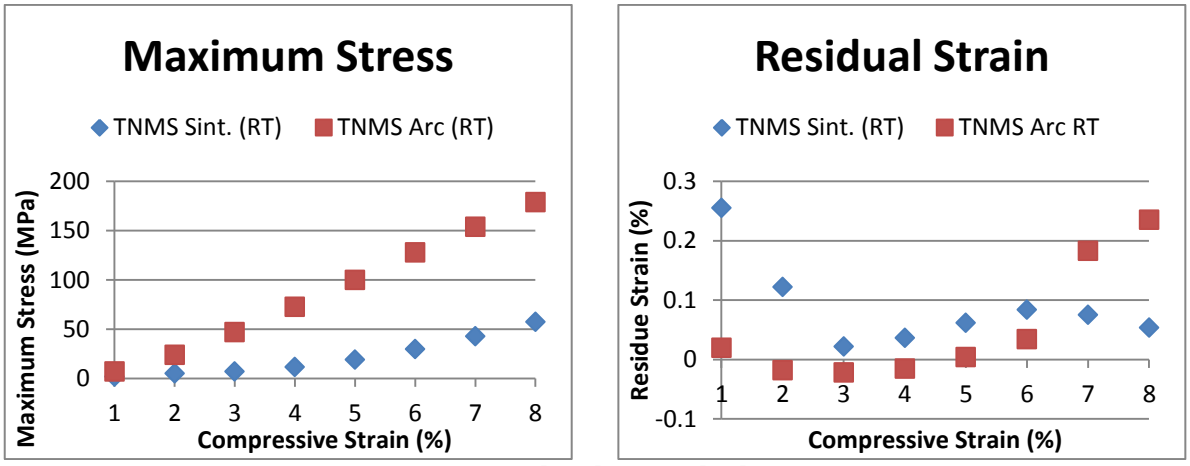

Figure 4.1 - TNMS sintered and arc-melted at room temperature

Note: - As residual strain is calculated from the difference between the initial loading strain value and the final unloading strain value, a negative value is an anomaly generated by the alloy still being loaded from after the last cycle, thus giving the initial load strain a larger value and should accordingly be discounted from results.

Figure 4.1 above is the stress-strain results from 1-8% compressive strain at constant room temperature. The arc-melted alloy is shown to exhibit superior strength reaching approximately 180MPa in comparison to the sintered alloy which reaches approximately 60MPa at 8% compressive strain.

The sintered alloy shows an initial large residual strain followed by a gradual decrease after each compressive strain cycle. The arc-melted alloy shows the opposite behaviour with a gradual increase of residual strain thereafter. On average at each compressive strain, the sintered alloy reaches ~8.9% and arc-melted alloy reaches ~9.5% from its original shape.

4.2 Compressive strain at <14°C results

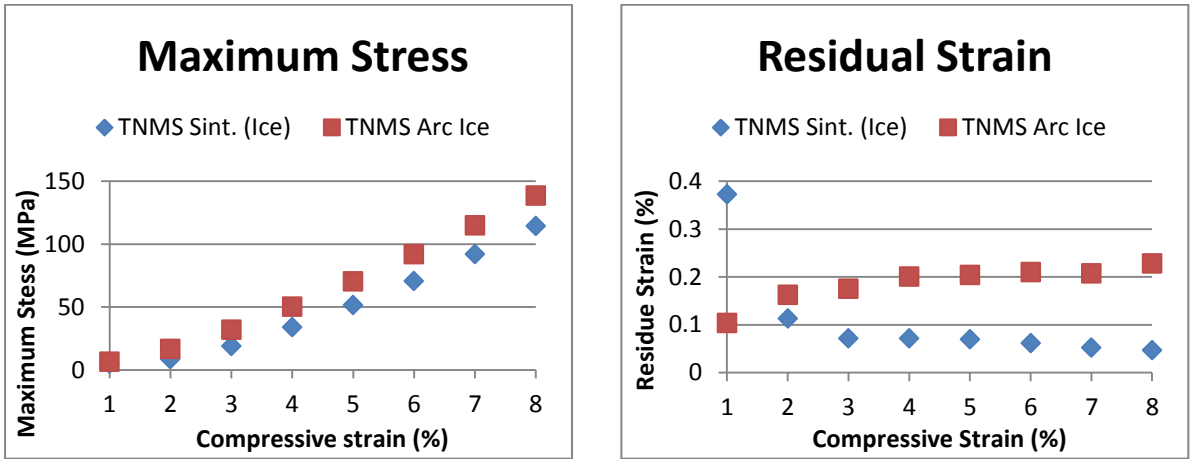

Figure 4.2 - TNMS sintered and arc-melted at <14°C

Figure 4.2 above is the stress-strain results from 1-8% compressive strain at temperatures just slightly lower than 14°C. Both alloys have similar maximum stresses with the arc-melted alloys reaching slightly higher maximum stress of approximately 140MPa and sintered reaching approximately 120MPa at 8% compressive strain. The sintered alloy becomes more elastic with each strain cycle and the arc-melted becomes less elastic. On average, the sintered alloy reaches ~10.7% and arc-melted alloy reaches ~18.6% from its original shape.

4.3 Compressive strain at human body temperature results

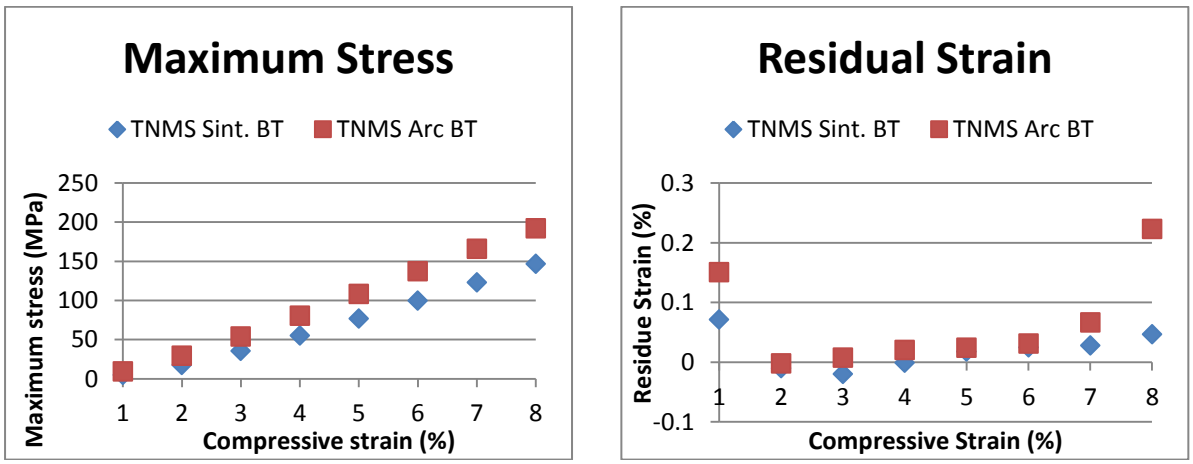

Figure 4.3 - TNMS sintered and arc-melted at human body temperature

Figure 4.2 - TNMS sintered and arc-melted at <14°C

Figure 4.3 above is the stress-strain results from 1-8% compressive strain at human body temperature. Both alloys have similar maximum stresses with the arc-melted alloys reaching slightly higher maximum stress of approximately 195MPa and sintered reaching approximately 150MPa at 8% compressive strain. Deviating from the previous temperatures, the arc-melted alloy becomes more elastic with each strain cycle as well as the sintered alloy. On average, the sintered alloy reaches ~3.8% and arc-melted alloy reaches 7.5% from its original shape.

4.4 Compressive strain at >50°C results

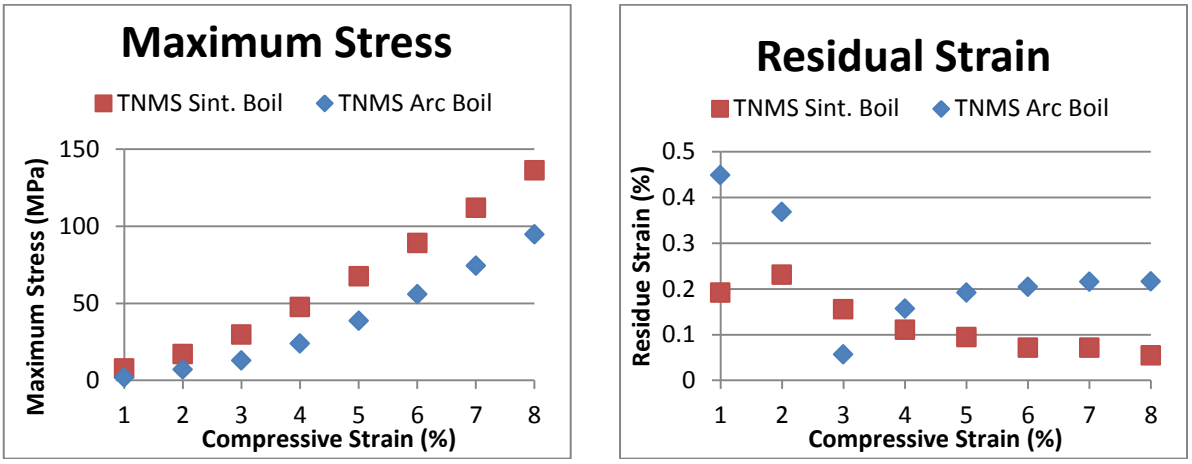

Figure 4.4 - TNMS sintered and arc-melted at >50°C

Figure 4.4 above is the stress-strain results from 1-8% compressive strain at temperatures just slightly higher than 50°C. These results show that the sintered alloy achieves a higher maximum stress at approximately 140MPa and arc-melted reaching lower maximum stress of approximately 95MPa at 8% compressive strain. The sintered alloy again becomes more elastic with each strain cycle and the arc-melted alloy becoming less elastic. On average, the sintered alloy reaches ~12.3% and arc-melted alloy reaches 23.2% from its original shape.

4.5 Sintered TNMS increasing loads, constant temperature

Sintered TNMS alloys were given different loads in increments of 500N from 500-2.5kN at constant temperature and stress-strain curves recorded for each load. Shown in Figure 4.5 below, at lower temperatures, there is hysteresis as the alloy is loaded and unloaded at the same constant temperature, however, at 25-30°C the hysteresis is almost non-existent as the alloy almost returns exactly upon itself during unloading. The hysteresis builds up again the higher the temperature moves away from 30°C.

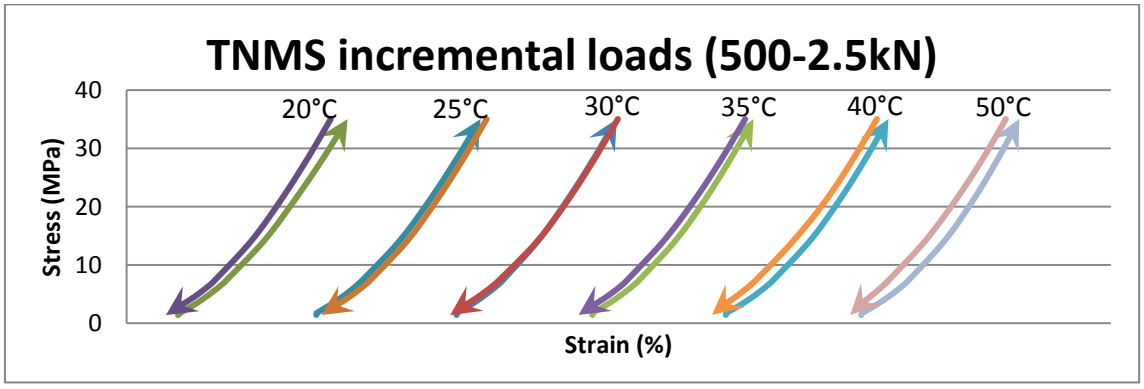

Figure 4.5 - TNMS incremental loads, constant temperature

4.6 Sintered TNMS constant load, varying temperatures

Keeping the load constant and changing the temperatures (increasing past 50°C), an interesting spike in strain can be observed around the 24-26°C mark on cooling the alloy at the constant 1.5kN load applied as shown by Figure 4.6 below.

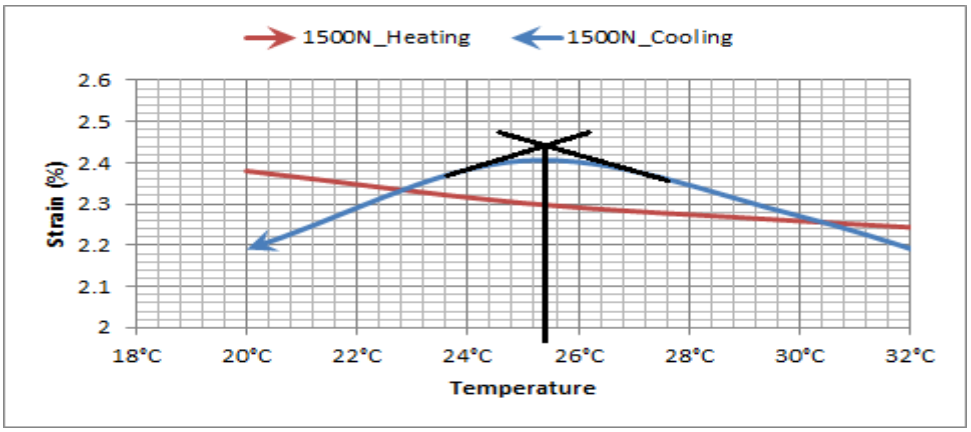

Figure 4.6 - TNMS constant load, varying temperatures

4.7 Sintered alloy Nb composition change at room temperature

Table 3 - Niobium composition data

Alloy name	Composition (at.%)	Height (mm)	Diameter (mm)
5Nb	Ti-5Nb-4Mo-1Sn	6.47	9.7
7.5Nb (TNMS)	Ti-7.5Nb-4Mo-1Sn	6.49	9.61
10Nb	Ti-10Nb-4Mo-1Sn	7.93	9.93

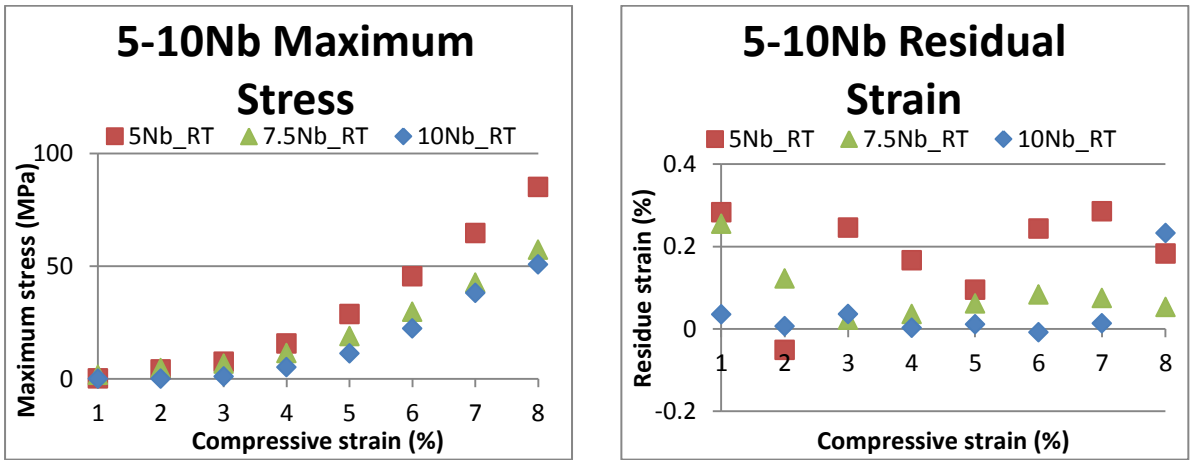

Figure 4.7 - 5-10Nb alloys at room temperature

Figure 4.7 above shows that the lower amount of Nb is able to achievable higher maximum stresses of approximately 90MPa with the opposite effect with higher amounts of Nb achieving lower maximum stresses of approximately 50MPa at 8% compressive strain. The average residual strains for each compressive load shows that the lower amount of Nb has an

average residual strain of ~21.5% and again the opposite effect with higher amounts of Nb which has an average residual strain of ~4.8%.

At constant load and changing the temperatures, a spike in strain can be observed from Figure 4.8 below, around 30-32°C in the 10Nb alloy at 1.5kN load as the temperature increases.

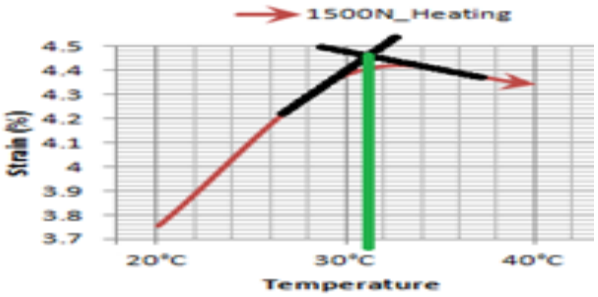

Figure 4.8 - 10Nb heating spike

4.8 Sintered alloy Mo composition change at room temperature

Table 4 - Molybdenum composition data

Alloy name	Composition (at.%)	Height (mm)	Diameter (mm)
2Mo	Ti-7.5Nb-2Mo-0.5Sn	6.75	9.69
4Mo (TNMS)	Ti-7.5Nb-4Mo-1Sn	6.49	9.61
6Mo	Ti-7.5Nb-6Mo-2Sn	6.44	9.8

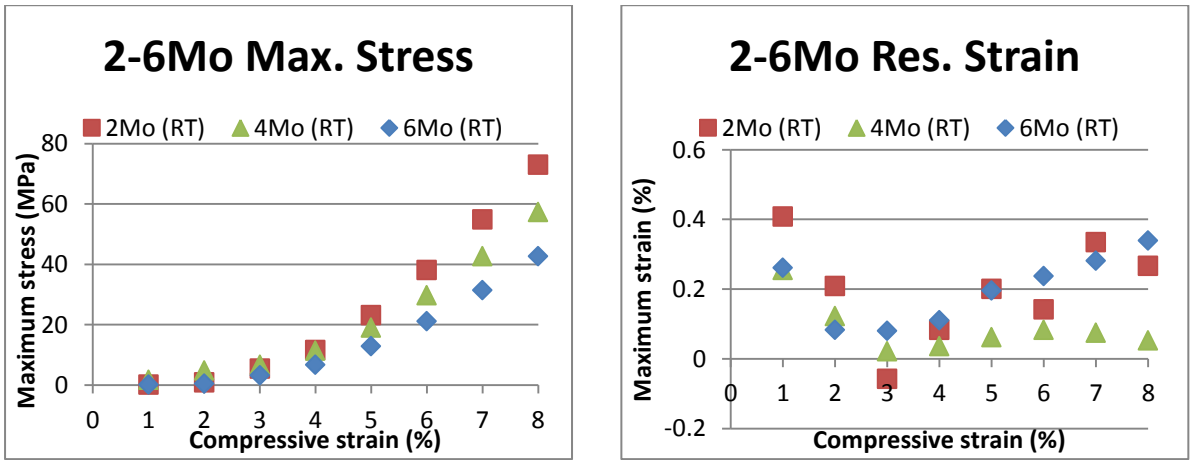

Figure 4.9 - 2-6Mo alloys at room temperature

Figure 4.9 above shows that the lower amount of Mo makes the alloy stronger, reaching higher maximum stresses of 75MPa with the opposite effect with higher amounts of Mo achieving lower maximum stresses of approximately 40MPa at 8% compressive strain. The average residual strains for each compressive load shows that the lower amount of Mo has an average residual strain of ~23.5% and again the opposite effect with higher amounts of Mo which has an average residual strain of ~19.9%.

At constant loads and changing the temperatures, a spike in strain can be observed from Figure 4.10 below around 30-32°C in the 6Mo alloy at 1.5kN load as the temperature increases.

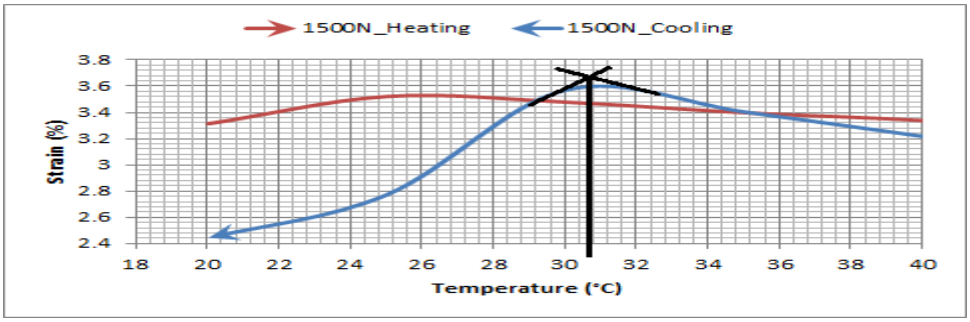

Figure 4.10 - 6Mo cooling spike

4.9 Sintered alloy Sn composition change at room temperature

Table 5 - Tin composition data

Alloy name	Composition (at.%)	Height (mm)	Diameter (mm)
0.5Sn	Ti-7.5Nb-4Mo-0.5Sn	6.07	9.69
1Sn (TNMS)	Ti-7.5Nb-4Mo-1Sn	6.49	9.61
2Sn	Ti-7.5Nb-4Mo-2Sn	6.94	9.59

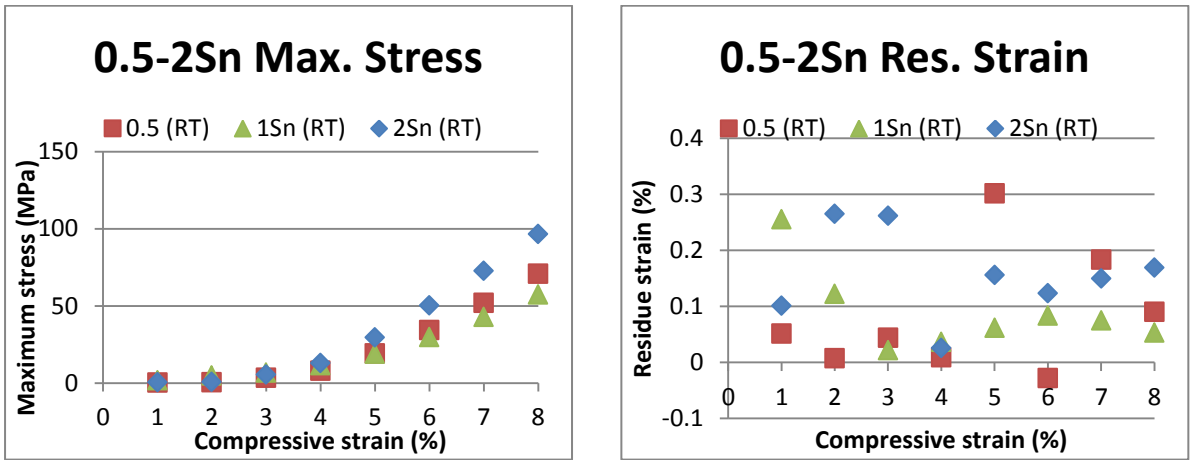

Figure 4.11 - 0.5-2Sn alloys at room temperature

Figure 4.11 above shows that the lower amount of Sn is has a maximum stress in-between the higher amounts of Sn. 1Sn alloy is shown to achieve the lowest maximum stress of approximately 50MPa, with 0.5Sn achieving approximately 70Mpa and 2Sn approximately 95MPa at 8% compressive strain. The average residual strains for each compressive load shows that the lower amount of Sn has an average residual strain of ~8.2% and higher amounts of Sn which has an average residual strain of ~15.6%.

5 DISCUSSION OF RESULTS

The following section will details the development procedures further, giving particular scope to any issues encountered.

5.1 Sintering

The time taken to ramp the alloys temperature from room temperature (~20°C) to 1000°C, at a rate of 5°C per minute meant the ramping up temperature took roughly 196 minutes and when combined with the 180 minute dwell period, the time elapsed was roughly 376 minutes. The ramp down from 1000°C to room temperature at a rate of 35°C per minute theoretically would have taken 28 minutes, however, it was found that this time was only for the heating element to cool down to 20°C; the actual alloys took a further, ~180 minutes to cool down to 20°C, which the time and temperatures subjected when cooling down acted as a heat-treatment for the sintered alloys. This further heat-treatment of the sintered alloys could have promoted additional phase changes within the sintered alloy and explain some of the results shown above as the arc-melted alloy did not have a further heat-treatment. Figure 5.1 below shows the comparison of theoretical and actual sintering.

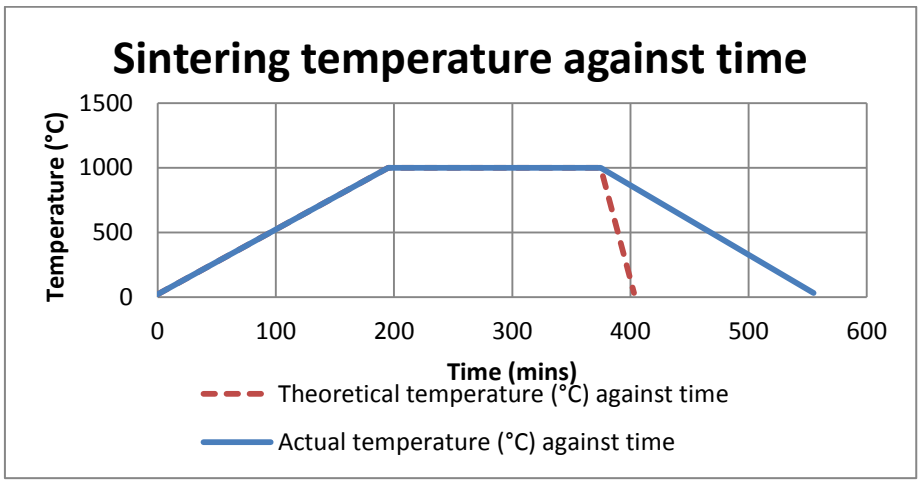

Figure 5.1 - Sintering temperature with time

5.2 Arc-melting

During arc-melting, it was noted that after the first melt, a significant amount of the sample had evaporated, coating the chamber in a thin layer of powder. This led to the suggestion that arc-melting may be too harsh a fusion process to melt the alloys. However, with the second melt, at a higher current, there was no loss from the sample, but this may be due to the alloy already being fused together rather than the first melt not being adequate.

Arc-melting was a significantly faster fusion process; where sintering was around 10 hours to complete, arc-melting was roughly only 1 hour. The actual melting of the alloy took only a few seconds for the discharge to melt this alloy, because the alloy is melted at a much higher temperature than sintering; where with sintering the temperature can be more controlled, but when arc-melting the temperature can reach significantly higher than 1000°C in the matter of

seconds. Figure 5.2 below shows the theoretical arc-melting temperature with time, against the sintering temperature with time.

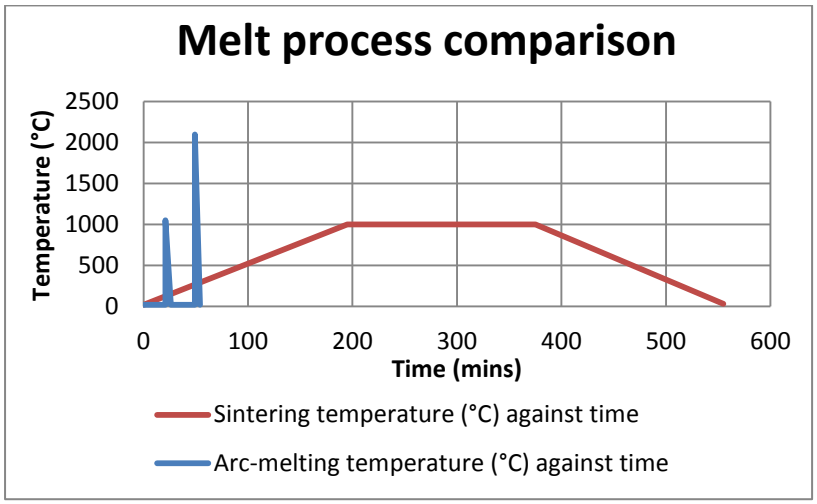

NOTE:-
(Arc-melted temperatures are purely hypothetical for comparison in fusion process).

Figure 5.2 - Fusion melt comparison

5.3 X-ray diffraction

Samples of TNMS powders before and after milling as well as sintered and arc-melted alloys were submitted for X-ray diffraction (XRD) analysis. XRD profiles would determine the phase changes that occurred (α->β). XRD analysis was conducted at room temperature. XRD profiles referred to below are shown in APPENDIX B.

5.3.1 Powder milling XRD profiles

Figure 0.1 shows the TNMS composition powder sample before milling. β and α-phase are noted with predominantly more α-phase. Figure 0.2 shows the powders after milling for 18 hours, where high β-phase peaks were noted with low α-phase peaks which agrees with literature [11] which states longer milling time would promote more β-phase change.

5.3.2 Sintered and arc-melted XRD profiles

Figure 0.3 shows the sintered alloy shows several α-phase peaks but with higher β-phase peaks. Figure 0.4 shows the arc-melted alloy shows much less α-phase than the sintered and significantly higher peaks of β-phase.

An assumption could be made that arc-melting is the better technique to employ for phase changes. However, the sintered profile shows Nb and Mo peaks, whereas arc-melted shows only Nb. This could be down to two reasons: the Mo was dissolved into the Ti-based alloy during arc-melting and therefore arc-melting would be the better technique, or as previously stated, a significant amount of the powders evaporated during first melting of the arc-melted alloy, which could have been the Mo element of the alloy; if so, then arc-melting may not be the better technique. Regardless of this, it is shown from both profiles, β-phase are from Nb peaks which would mean Nb is the better β-stabilising element.

5.4 Mechanical test results

The following tables below are the summation of the mechanical test results for sintered and arc-melted alloys and composition changes. Maximum stress is taken from the 8% compressive strain results and residual strain is calculated from the average of each compressive strain.

Note: - It should be noted here that due to the evaporation of material in the arc-melted alloys, it may not be safe to say these alloys are the same in composition, so the following results may not be comparable.

Table 6 - Sintered & Arc-melt result data

Name	Composition (at.%)	Temperature	Maximum stress (MPa)	Residual strain (%)
TNMS Sint.	Ti-7.5Nb-4Mo-1Sn	<14°C	115	10.7
TNMS Sint.	Ti-7.5Nb-4Mo-1Sn	Room	60	8.9
TNMS Sint.	Ti-7.5Nb-4Mo-1Sn	Human body	145	3.8*
TNMS Sint.	Ti-7.5Nb-4Mo-1Sn	>50°C	135	12.3
TNMS Arc.	Ti-7.5Nb-4Mo-1Sn	<14°C	140	18.6
TNMS Arc.	Ti-7.5Nb-4Mo-1Sn	Room	180	9.5
TNMS Arc.	Ti-7.5Nb-4Mo-1Sn	Human body	190	7.5
TNMS Arc.	Ti-7.5Nb-4Mo-1Sn	>50°C	95	23.2

* The average residual strain of the human body temperature alloy had very erroneous results so should probably be disregarded with these results.

Overall, arc-melted alloys are capable of reaching higher stresses at the varying temperatures with exception of over 50°C and are quite drastically different to the sintered alloys. With regards to the elastic properties of the alloys from the residual strains, the sintered alloy proves to be more elastic than the arc-melted alloy at all temperatures due to the lower residual strains after load/ unloading.

An assumption for the differences is that, with the sintered alloys, the fusion process (as it was not a uniform melt due to the different element melting points) may have created small pores within the alloy, in which the alloy would not be completely solid, so any tests would reflect that as structurally with the pores it is weaker. The arc-melted alloys would be the complete opposite, the fusion process (as it was quite violent) may have melted all elements above their melting points in a fraction of a second ensuring everything melted simultaneously, in which the alloy would therefore be more of a complete solid and therefore stronger: hence the higher stresses achieved.

Another assumption for the differences is due to the temperatures applied: the alloys may be exhibiting shape memory properties. Transformation temperatures may present in the results in particular shown by the sintered alloy, which was designed to exhibit shape memory properties at room temperature, the low residual strains at room temperature as the alloy becomes more elastic reflects this. The arc-melted alloy also was designed to have shape memory properties at room temperature, but instead seems to start showing low residual strains at human body temperature instead: this could be due to the composition issues.

The incremental loading at constant temperature results for the sintered alloy shown in Figure 4.5 showed hysteresis in the alloy as it was loaded and unloaded at temperatures lower and greater than 25-30°C; room temperature. This would also refer to the transformation temperatures affecting the alloy at these temperatures with the alloy becoming more elastic due to the low hysteresis. Similar results are noted when keeping constant loads and changing the temperatures for the sintered alloy, Figure 4.6 notes a spike around the 24-26°C upon cooling. This may mean the Ms temperature of the alloy is around these temperatures which coincides with literature [3].

5.4.1 Comparison of sintered niobium alloy compositions

Table 7 - Niobium result data

Name	Composition (at.%)	Temperature	Maximum stress (MPa)	Residual strain (%)
5Nb	Ti-5Nb-4Mo-1Sn	<14°C	75	13
7.5Nb (TNMS)	Ti-7.5Nb-4Mo-1Sn	<14°C	115	10.5
10Nb	Ti-10Nb-4Mo-1Sn	<14°C	70	16.7
5Nb	Ti-5Nb-4Mo-1Sn	Room	85	21.5
7.5Nb (TNMS)	Ti-7.5Nb-4Mo-1Sn	Room	55	8.9
10Nb	Ti-10Nb-4Mo-1Sn	Room	50	4.8

At temperatures slightly less than 14°C, 5Nb and 10Nb achieve similar maximum stresses and 7.5Nb reaches the largest maximum stress. As the Nb amount increases, with exception to 7.5Nb, the alloy becomes less elastic. At room temperature, as the Nb amount increases, the maximum stresses and residual strains decrease.

It is possible that 5Nb has quite a low transformation temperature range, with Ms lower than 14°C. This is due to the alloy becoming harder and less elastic as the temperature increases. 7.5Nb and 10Nb show the biggest change as the temperature increases, both becoming softer and more elastic. This is expected with the 7.5Nb alloy which is supposed to have shape memory properties at room temperature, but it is also a sign of β-phase forming at these temperatures as the higher amount of Nb in the 10Nb becomes even more elastic and is more likely to show shape memory properties at these temperatures.

Figure 4.8 shows the 10Nb alloy as it is heat up whilst the load applied is kept constant. A spike in strain is generated around 30-32°C and due to the fact the alloys temperature is increasing when this spike occurs it could be assumed that this could be the lower end Af characteristic of the 10Nb alloys transformation temperature. This, alongside the fact the alloy is showing no sign of shape memory properties at lower temperatures, could be signs that Nb has shifted the temperature transformation characters above the original room temperature values by the addition of Nb.

5.4.2 Comparison of sintered molybdenum alloy compositions

Table 8 - Molybdenum result data

Name	Composition (at.%)	Temperature	Maximum stress (MPa)	Residual strain (%)
4Mo (TNMS)	Ti-7.5Nb-4Mo-1Sn	<14°C	115	10.5
6Mo	Ti-7.5Nb-6Mo-1Sn	<14°C	90	19.4
4Mo (TNMS)	Ti-7.5Nb-4Mo-1Sn	Room	55	8.9
6Mo	Ti-7.5Nb-6Mo-1Sn	Room	40	19.9
4Mo (TNMS)	Ti-7.5Nb-4Mo-1Sn	Human body	145	3.8*
6Mo	Ti-7.5Nb-6Mo-1Sn	Human body	130	9.2
4Mo (TNMS)	Ti-7.5Nb-4Mo-1Sn	>50°C	135	12.2
6Mo	Ti-7.5Nb-6Mo-1Sn	>50°C	85	21.2

At temperatures lower than 14°C, 4Mo and 6Mo alloys are shown to be quite strong and not very elastic. At room temperature, 4Mo starts to exhibit shape memory properties as expected, whereas although 6Mo becomes weaker reaching lower maximum stress, it becomes even more inelastic. At human body temperature, a significant change is noted in 6Mo as the residual strain decreases. At temperatures greater than 50°C, both 4Mo and 6Mo alloys become stronger and less elastic.

It is possible that the Mo amount is having a significant effect on the elasticity of the alloys, as 4Mo becomes very elastic at room temperature from all other temperatures and 6Mo becomes very elastic around human body temperature. As Mo is a β-stabiliser, Mo amount here seems to be changing the transformation temperatures, although not as much as Nb.

Figure 4.10 shows 6Mo as it is cooled down whilst keeping the load applied constant. A spike in strain is generated around 30-32°C and due to the fact the alloys temperature is decreasing when this spike occurs it could be assumed that this could be the M_S characteristic of this alloys temperature transformation. This, alongside the fact the alloy is showing no sign of shape memory properties at lower temperatures (at least in terms of elasticity), could be signs that Mo has also shifted the temperature transformation characters above the original room temperature values by the addition of Mo.

5.4.3 Comparison of sintered tin alloy compositions

Table 9 - Tin result data

Name	Composition (at.%)	Temperature	Maximum stress (MPa)	Residual strain (%)
0.5Sn	Ti-7.5Nb-4Mo-0.5Sn	Room	70	8.2
1Sn (TNMS)	Ti-7.5Nb-4Mo-1Sn	Room	55	8.9
2Sn	Ti-7.5Nb-4Mo-2Sn	Room	95	15.6

Literature has stated that Sn should have very little effect on shape memory properties for alloys but instead is used in alloys to strengthen them without embrittlement [11]. This is seen from the Sn results, as when Sn increases, the alloy becomes harder (larger maximum stress) and less elastic.

6 CONCLUSION AND FUTURE WORK

The previous described the development process of replicating a Ti-7.5Nb-4Mo-1Sn (TNMS) alloy which was found by [3] to exhibit shape memory properties; transformation temperatures, superelasticity (SE) and shape memory effect (SME), around room temperature (20-25°C). Experimentation through changes in the composition and development of the TNMS alloy was conducted to make the alloy exhibit these shape memory properties at body temperature (37°C) for the alloy to be used in medical devices.

Literature has shown that homogenisation through ball milling prior to fusion has an effect on promoting β-phase changes in Ti-based powders, which from X-ray diffraction (XRD) profiles of the TNMS powders after milling shows an increase of β-phase.

Two fusion techniques were used to create the alloys, sintering and arc-melting. Through compressive mechanical testing the sintered alloy exhibited shape memory properties at room temperature similar to literature [3]. Through incremental loading at constant temperature, close to zero hysteresis was noted in the sintered alloys at 25-30°C. Through constant loading at varying temperatures, a spike is noted on cooling graph of the sintered alloy around 24-26°C which may be the Ms temperature of the alloy.

The arc-melted alloys did not exhibit these properties at room temperature, but instead started to show changes in properties at human body temperature and in particular more elasticity at temperatures >50°C. However, due to evaporation of material during arc-melting, the composition of arc-melted alloys may not have been similar to the composition of the sintered alloys, so comparison may not reflect the true results.

Nb was shown to have had the greatest effect on shape memory properties due to how elastic the alloys behaved. Transformation temperatures were shown to have been effected through changing Nb, where 10Nb showed possible Af characteristics around 30-32°C.

Mo was shown to have similar effects on shape memory properties although not as much as Nb. Transformation temperatures however were shown to be very different in the higher amount of Mo with a shift of ~5°C to 30°C possible Ms characteristic from the original TNMS alloy. Mo seems to have a bigger effect on the elasticity of the alloys having the lowest residual strain, or returning closest to the original form before loading.

The Sn element was shown to have a strengthening effect on the alloy, with higher context making the alloy much stronger than any of the other alloy compositions. When dealing with medical devices there will be a need to have a strong material due to possible applications (like if incorporated into leg prosthesis) or in case of any damage done to the device.

For purposes of the application for this thesis, a Ti-based alloy with higher amounts of Nb and Mo would be best for dictating transformation temperatures close to body temperature with the desired SME to allow for expansion, with 10Nb having the alloys transformation temperatures start in the 30°C range and 6Mo making the alloy more superelastic.

6.1 Future work

All different alloy compositions should be created and tested for an overall picture of the effects each element has on mechanical properties, as well as results with erroneous data should be retested.

All current tests have been carried out using compressive strain testing due to current moulds. Creation of the universal mould to allow for tensile and destructive tests to be carried out examining full mechanical properties, such as yield stresses, failure and elongation, etc.

Energy-dispersive x-ray spectroscopy (EDX) should be used to determine the actual composition of the alloys before testing. *In-situ* TEM (Transmission Electron Microscopy) should be used to give more scope to the shape memory effects of the alloy through images of the crystal changes during loading/ unloading.

Once the correct composition and development process has been derived the alloy should respond to human body temperature by expanding. However, external temperatures could start this process prematurely so an overall control system has also be in place to only allow the alloy to expand through use of human body temperature: an energy harvesting system.

The system must allow only human body temperature to affect the alloy, so it is possible the alloy would be housed within the harvest system. A rough possible idea to allow this system to carry out this function would be to shield the alloy from all external temperatures completely, so the harvest system would need to be insulated: so long as the alloy does not reach over its M_S value it would not act as a shape memory alloy. The harvest system would require a processor that an algorithm would be programmed onto and when the algorithm reached a certain state a signal could be passed to the system to allow heat to pass through/ pass into the system and onto the alloy. The heat passing could be done via a small hatch/ opening that would open on the system, allowing the heat to rise from the body into the system and consequently to the alloy, which would start the process of the alloy expanding.

7 ACKNOWLEDGEMENTS

The author would like to thank Dr. Carmen Torres-Sanchez and Dr. Theodore Lim for their support and knowledge contributed towards this project and acknowledge other staff members from Heriot-Watt University, including Dr. Jan-Willem Bos, Ruth Downie for help with arc-melting and Dr. David Gow from Edinburgh Southeast Mobility and Rehabilitation Technology (SMART) centre.

Finally the author would like dedicate this thesis to, and thank his partner, Kim McBeth, for her morale support and advice throughout the project: without her, this project would not have been possible.

8 REFERENCES

1. Wong, L. *Temperature of a Healthy Human (Body Temperature)*. 1997 [cited 2012; Available from: http://hypertextbook.com/facts/LenaWong.shtml.
2. Dictionary, T.A.H. *Room Temperature*. 2009 [cited 2012; Fourth:[Available from: http://www.thefreedictionary.com/room+temperature.
3. Zhang, D.C., et al., *Shape memory and superelastic behavior of Ti-7.5Nb-4Mo-1Sn alloy.* Materials & Design, 2011. **32**(8-9): p. 4614-4617.
4. Pio John S. Buenconsejo, H.Y.K., Hideki Hosoda, Shuichi Miyazaki, *Shape memory behavior of Ti-Ta and its potential as a high-temperature shape memory alloy.* Acta Materialia, 2009. **57**: p. 1068-1077.
5. F. Nozoe, H.M., T. K. Jung, S. Watanabe, T. Saburiand S. Hanada, *Effect of Low Temperature Aging on Superelastic Behavior in Biocompatible B TiNbSn Alloy.* Materials Transactions, 2007. **48**(11): p. 3007 to 3013.
6. B.V., L. *Chemical properties of nickel - Health effects of nickel*. [cited 2014; Available from: http://www.lenntech.com/periodic/elements/ni.htm.
7. Registry, A.f.T.S.a.D. *2. RELEVANCE TO PUBLIC HEALTH*. [cited 2014; Available from: http://www.atsdr.cdc.gov/toxprofiles/tp15-c2.pdf.
8. Hiroyasu Kanetaka, H.H., Yoshinaka Shimizu, Tada-aki Kudo, Ye Zhang, Mitsuhiro Kano, Yuya Sano, Shuichi Miyazaki, *In Vitro Biocompatibility of Ni-Free Ti-Based Shape Memory Alloys for Biomedical Applications.* Materials Transactions, 2010. **51**(10): p. 1944 to 1950.
9. Hee Young Kim, H.S., Jae Il Kim, Hideki Hosoda, Shuichi Miyazaki, *Mechanical Properties and Shape Memory Behavior of Ti-Nb Alloys.* Materials Transactions, 2004. **45**(7): p. 2443 to 2448.
10. S. Miyazaki, Y.O., K. Otuska, Y. Suzuki, *C4.* J. de Physique, 1982: p. 255-260.
11. A. M. Omran, K.D.W., D. K. Kim, S. W. Kim, M. S. Moon, N. A. Barakat and D. L. Zhang, *Effect of Nb and Sn on the Transformation of α-Ti to β-Ti in Ti-35Nb-2.5 Sn Nanostructure Alloys using Mechanical Alloying.* Metals and Materials International, 2008. **14**(3): p. 321-325.
12. T. Maeshima, S.U., K. Yamauchi, M. Nishida, *Effect of heat treatment on shape memory effect and superelasticity in Ti-Mo-Sn alloys.* Materials Transactions, 2006: p. 844-847.
13. T. Maeshima, M.N., Materials Transactions, 2004. **45**: p. 1096-1100.
14. D.C. Zhang, J.G.L., W.J. Jiang, M. Ma, Z.G. Peng, *Shape memory and superelastic behavior of Ti-7.5Nb-4Mo-1Sn alloy.* Materials and Design, 2011. **32**: p. 4614-4617.
15. Nouri, A., P.D. Hodgson, and C. Wen, *Effect of ball-milling time on the structural characteristics of biomedical porous Ti-Sn-Nb alloy.* Materials Science and Engineering C, 2011. **31**(5): p. 8.
16. FRITSCH. *PLANETARY MILLS Operating Manual*. 2005 [cited 2012 16/04]; 03/205:[Available from: http://www.fritsch-milling.com/uploads/tx_downloads/BA_062000_1336_e_01.pdf.
17. Torres-Sanchez, C., *Softer on the bones: Superelastic and very low Young's Modulus for TiNbSn alloy for bone grafts*, 2012, Heriot Watt University: Material Science and Engineering C.

APPENDIX A

Table 10 - Metal characteristics

Metal	**Symbol**	**Atomic weight**
Titanium	Ti	47.8670
Niobium	Nb	92.9064
Molybdenum	Mo	95.9600
Tin	Sn	118.7100

Example, for Ti element of, 87.5Ti-7.5Nb-4Mo-1Sn, from (at.%) to (wt.%):

Equation 1 - Ti (at.%) to (wt.%) example

$$\frac{87.5 * 47.8670}{(7.5 * 92.9064) + (4 * 95.96) + (1 * 118.71)} . 100\% = 77.7392$$

Example, for Ti from (wt.%) to weight of a 4gram sample:

Equation 2 - Ti (wt.%) to weight example

$$\frac{77.7392}{100\%} * 4 = 3.1096g$$

Desired (at.%) to (wt.%) to weight of a 4g, Ti-7.5Nb-4Mo-1Sn alloy:

Table 11 - Desired composition

								Total
(at.%)	**87.5000**	**Ti**	**7.5000**	**Nb**	**4.0000**	**Mo**	**1.0000**	**Sn**	**100%**
(wt.%)	77.7392	Ti	12.9331	Nb	7.1244	Mo	2.2033	Sn	100%
Weight	3.1096g	Ti	0.5173g	Nb	0.2850g	Mo	0.0881g	Sn	4.0000g

Actual weight to (wt.%) to (at.%) of a 4g, Ti-7.5Nb-4Mo-1Sn alloy:

Table 12 - Actual composition

								Total
Weight	3.1140g	Ti	0.5130g	Nb	0.2736g	Mo	0.0911g	Sn	3.9917g
(wt.%)	78.0119	Ti	12.8517	Nb	6.8542	Mo	2.2822	Sn	100
(at.%)	87.6808	Ti	7.4421	Nb	3.8428	Mo	1.0343	Sn	100

Amended weight to (wt.%) to (at.%) of a 4g, Ti-7.5Nb-4Mo-1Sn alloy:

Table 13 - Amended composition

									Total
Weight	3.1140g	Ti	0.5157g	Nb	0.2873g	Mo	0.0911g	Sn	4.0081g
(wt.%)	77.6927	Ti	12.8664	Nb	7.1680	Mo	2.2729	Sn	100
(at.%)	87.4782	Ti	7.4640	Nb	4.0259	Mo	1.0319	Sn	100

Table 14 - Amendments required

(at.%)	-0.1808	Ti	0.0579	Nb	0.1572	Mo	-0.0343	Sn
(wt.%)	-0.1108	Ti	0.1081	Nb	0.2844	Mo	-0.0742	Sn
Weight	-0.0044g	Ti	**0.0043g**	**Nb**	**0.0114g**	**Mo**	-0.0030g	Sn

Molar model to convert (at.%) to weight.

Ti-7.5Nb-4Mo-1Sn = $Ti_{0.875}$-$Nb_{0.075}$-$Mo_{0.04}$-$Sn_{0.01}$

Multiply percent by atomic weight, then sum to get grams per mole:

Equation 3 - Grams per mole of alloy

$$(0.875 * 47.867) + (0.075 * 92.9064) + (0.04 * 95.9600) + (0.01 * 118.71) = 53.8771 g/mol.$$

Equation 4 - Molar value of sample

$$\frac{1}{53.8771} = 0.0186 mol.$$

To get weight percent (multiply by 100 for 100%):

- $Ti = 0.0186 * (0.875 * 47.867) = 0.7774$
- $Nb = 0.0186 * (0.075 * 92.9064) = 0.1293$
- $Mo = 0.0186 * (0.04 * 95.9600) = 0.0712$
- $Sn = 0.0186 * (0.01 * 118.71) = 0.0220$

Table 15 - Molar value results (left), mathematical value results (right) all in (wt.%)

Ti	=	77.7392%	Ti	=	77.74%
Nb	=	12.9331%	Nb	=	12.93%
Mo	=	7.1244%	Mo	=	7.12%
Sn	=	2.2033%	Sn	=	2.20%

.

APPENDIX B

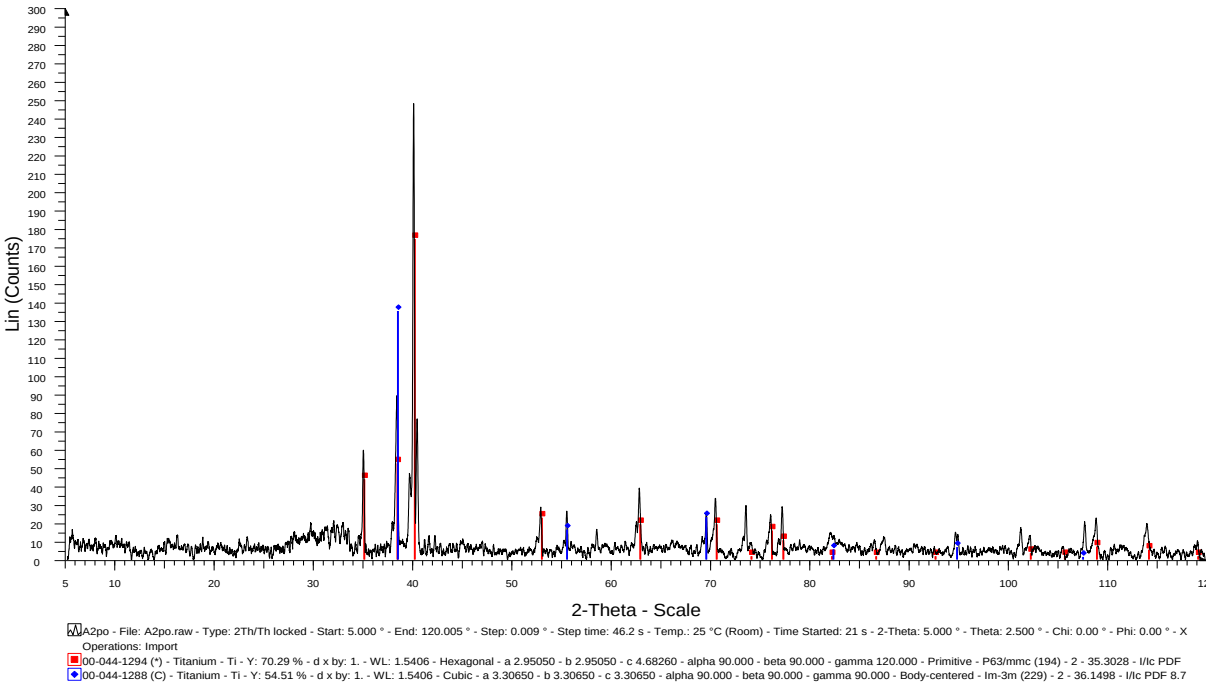

Figure 0.1 - Composition powders before milling

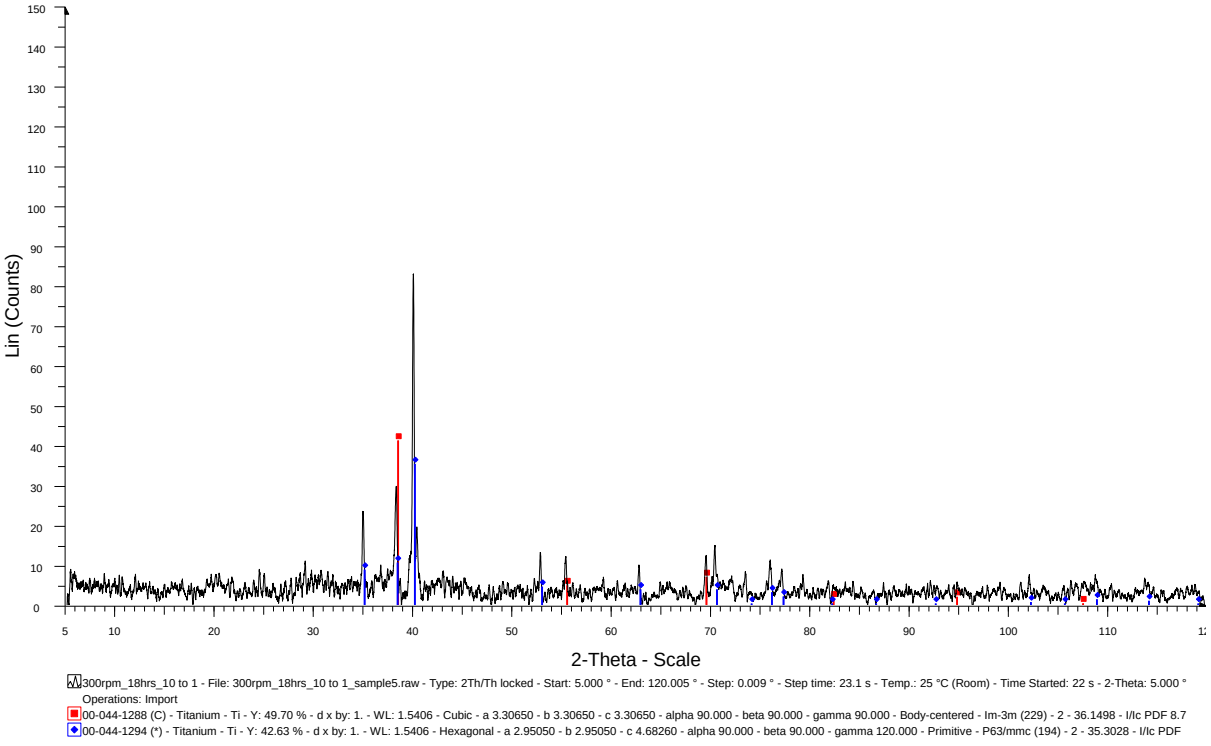

Figure 0.2 - Composition powders after milling

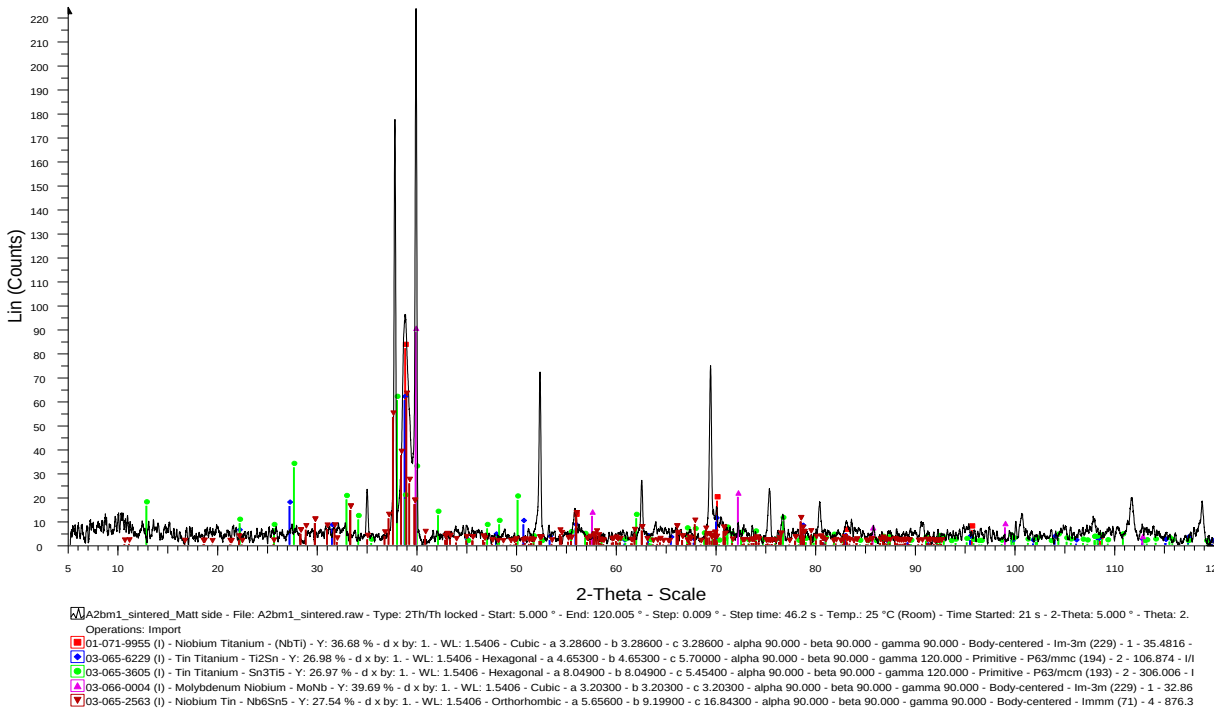

Figure 0.3 - Sintered TNMS profile

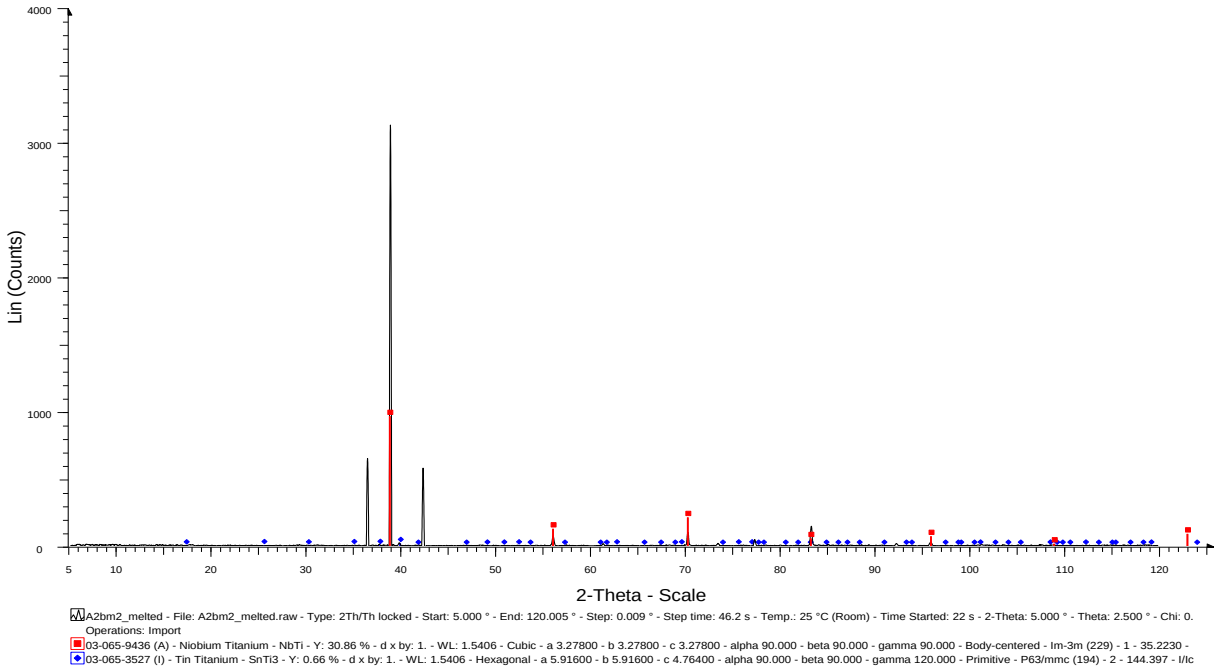

Figure 0.4 - Arc-melted TNMS profile